Oscillatory epidemic prevalence in growing scale-free networks

Yukio Hayashi, Masato Minoura, and Jun Matsukubo
Japan Advanced Institute of Science and Technology, Ishikawa 923-1292, Japan
(Received 5 February 2003; revised manuscript received 6 August 2003; published 28 January 2004)

We study the persistent epidemic prevalence with oscillatory behavior and the extinction of computer viruses via e-mails on a contact relational network growing with new users, for which scale-free structure is estimated from real data. Typical oscillatory phenomenon is simulated in a stochastic model for the execution and detection of viruses. The conditions of extinction by random and targeted immunizations for hubs are derived through bifurcation analysis for simpler deterministic models by using a mean-field approximation without the connectivity correlations. We can qualitatively understand the mechanisms of the spread in linearly growing scale-free networks.

DOI: 10.1103/PhysRevE.69.016112 PACS number(s): 05.65.+b, 87.23.Ge, 05.40.−a, 89.20.Hh

I. INTRODUCTION

In spite of different interactions between social, technological, or biological elements, many complex networks in real worlds have a common structure. It is based on a universal self-organized mechanism: network growth and preferential attachment of connections [1,2]. The structure is called scale-free (SF) network, which exhibits a power-law degree distribution $P(k) \sim k^{-\gamma}$, $2 < \gamma < 3$, for the probability of vertex with k connections. The topology deviates from the conventional homogeneous regular lattices and random graphs. Many researchers are attracted to a new paradigm of the heterogeneous SF networks in this active and fruitful area.

The structure of SF networks also has a strong impact on the dynamics of epidemic models for computer viruses, HIV, and others. Recently, it has been shown [3] that a susceptible-infected-susceptible (SIS) model on SF networks has no epidemic threshold; infections can be proliferated, whatever small infection rate they have. This result disproves the threshold theory in epidemiology [4]. The heterogeneous structure is also crucial for spreading the viruses on the analysis of susceptible-infected-recovered (SIR) models [5,6]. In contrast to the absence of epidemic threshold, an immunization strategy has been theoretically presented in a SIS model on SF networks [7,8]. The targeted immunization for the most highly connected vertices such as hubs applies the property of the extreme disconnections by attacks against the hubs [9] to a prevention against the spread of infections.

In this paper, we investigate the dynamic properties for spreading of computer viruses on the SF networks estimated from real data of e-mail communication [10]. As a new property in both simulation and theoretical analysis, we suggest that a growing network with new e-mail users causes the oscillatory prevalence recovered from a temporary silence of almost complete extinction. We refer to the typical oscillatory phenomenon in observations [11,12] as recoverable prevalence, which is not explained by the above statistical analyses at steady states or mean values (in the fixed size or $N \to \infty$). We first consider a realistic epidemic model on the growing SF network in simulations with the probabilistic execution and detection of viruses. Then, for understanding the mechanisms of such recoverable prevalence and extinction, we analyze simpler growing models in deterministic equations. By using a mean-field approximation without the connectivity correlations, we derive bifurcation conditions from the extinction to the recoverable prevalence (or the opposite), which is related to the growth, infection, and immune rates. Moreover, we verify the effectiveness of the targeted immunization for hubs by antiviruses even in the growing system.

II. E-MAIL NETWORK

A. The state transition for infection

We consider a network of contact relations whose vertices (nodes) and edges (links) correspond to computers and the communication via e-mails between users, respectively. Each vertex has two degrees, an in-degree for a received mail, which is the number of edges that point into the vertex, and an out-degree for a sent mail, which is the number pointing out. In the mailing processes, the state at each computer $i = 1, \ldots, N$ is changed from the susceptible, hidden, infectious, and to the recovered by the removal of viruses and installation of antiviruses. We make a realistic model in stochastic state transitions with probabilities of the execution and the detection of viruses. Figure 1 shows the state transitions, where λ and δ denote the execution rate from the hidden to the infectious state and the detection rate from the special subjects or doubtful attachment files. The probability of at least one detection from the n_i viruses on the computer is $1-(1-\delta)^{n_i}$, and the probability of at least one execution

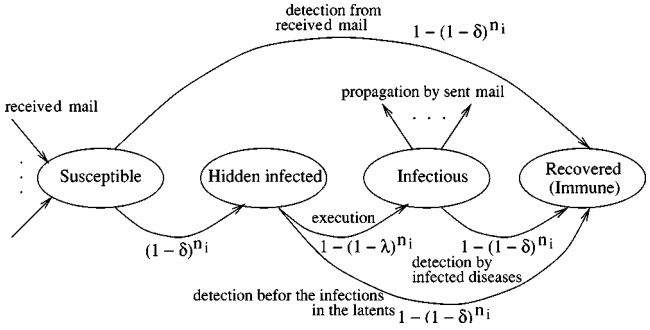

FIG. 1. S-H-I-R state transition diagram.

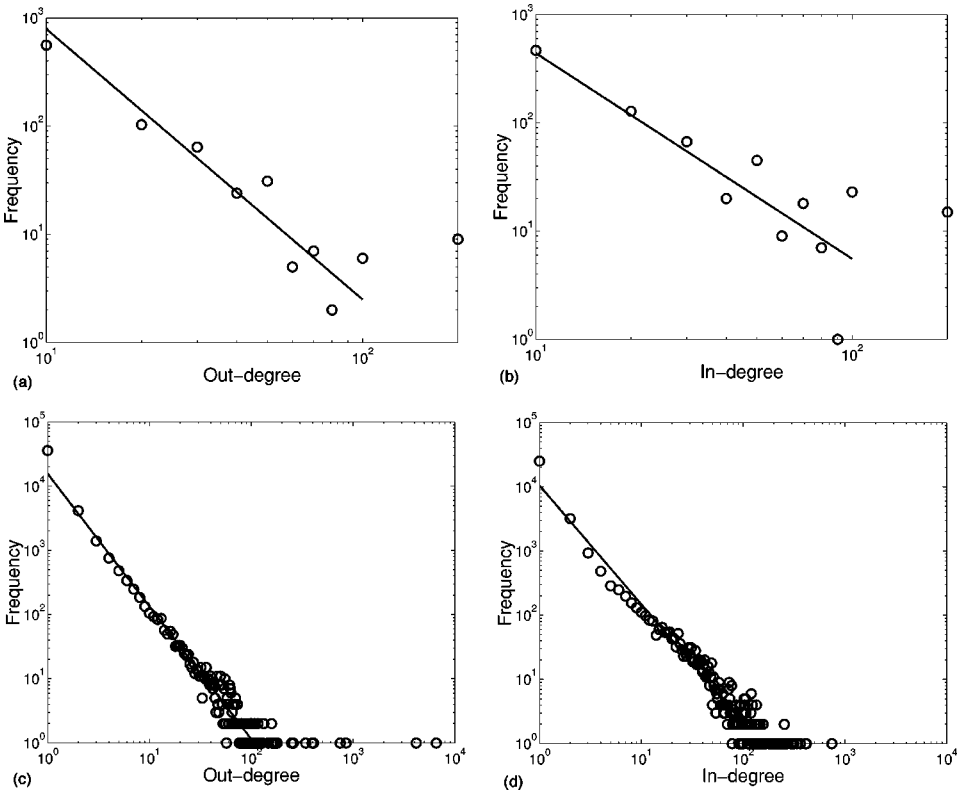

FIG. 2. Power-law degree distributions with the exponents $\gamma_{out}=2.5$ and $\gamma_{in}=1.9$ estimated for questionnaires of (a) sent mails and (b) received mails between users including the internal (measured users) and the external (other people) [10]. The frequency at degree k is counted in the interval between $[k,k+10]$, except for the outer of more than 100 degree at $k=200$. Similar distributions with (c) $\gamma_{out}=2.07$ and (d) $\gamma_{in}=1.85$ are estimated for the server log files of e-mails [13] including the internal and the external.

is $1-(1-\lambda)^{n_i}$. We assume the infected mail not sent again for the same communication partner (sent it at only one time) to be difficult for detection. Thus, n_i is at most the number of in-degree at each vertex. In the stochastic (susceptible–hidden infected–infections-recovered) SHIR model, the final state is the one recovered or immuned by antiviruses, if at least one infected mail is received.

B. The scale-free structure

We show the e-mail network structure based on real data measured by questionnaires for 2555 users in a part of World Internet Project 2000 [10]. The distributions of both sent and received mails follow a power law in Fig. 2(a), the exponents are estimated as $\gamma_{out}=2.5$, $\gamma_{in}=1.9$, and the average number of mails per day $\bar{k}=5-20$. These values are close to $\gamma_{out}=2.07$ and $\gamma_{in}=1.85$ estimated in the same range $1<k\leqslant 100$ for the server log files of e-mails [13] ($\gamma_{out}=2.03\pm0.12$ and $\gamma_{in}=1.49\pm0.12$ in Ref. [14]). There exists a slight difference between these estimated values which depend on the sample, measuring, and numerical precision. In addition, we have found that the cumulative histograms of less than degree k have similar shapes in a larger network of e-mail address books [15]. However, in the estimation for both data [10,13] by a stretched exponential function as in Ref. [15], the exponential parts almost vanish. Thus, the cumulative histograms are approximated by a power law as shown in Figs. 3(a) and 3(b). To discuss the delicate difference in the estimations for cumulative histograms is beyond

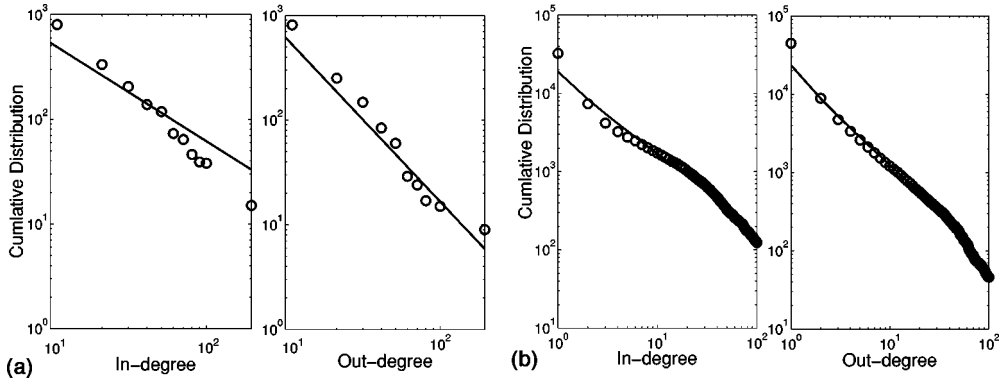

FIG. 3. The cumulative distributions of the in-degree and out-degree for e-mail networks in (a) the questionnaires [10] and (b) the server log files [13]. The linear fits are obtained by the integration of power-law functions estimated in Figs. 2(a–d) The misfit in the left-hand side of (a) is due to the dispersion in the limited size of data [10], especially around $k=100$ [see Fig. 2(b)].

TABLE I. Directed edge generation by the α-β coin.

Probability	α	$1-\alpha$
β	Self-loop at new vertex	Origin: new, terminal: old
$1-\beta$	Terminal: new, origin: old	Both of old vertices

the scope of this paper. It may be caused by the limited size of our sample.

C. The (α,β) model

We generate a SF network for the contact relations between e-mail users, by applying the simple (α,β) model [16] with the estimated exponents γ_{in} and γ_{out} in the preceding section. The slopes of power law $\gamma_{in} \approx 1/(1-\alpha)$ and $\gamma_{out} \approx 1/(1-\beta)$ are controlled by the α-β coin in Table I (in the case of e-mails $\alpha=0.4736$ and $\beta=0.6$). Growing with a new vertex at each step, k edges are added as follows. As the terminal, a coin toss chooses a new vertex with probability α and an old vertex with probability $1-\alpha$ in proportion to its in-degree. As the origin, the coin chooses a new vertex with probability β and an old vertex with probability $1-\beta$ in proportion to its out-degree. According to both the growth and the preferential attachment [1,2], the generation processes are repeated until the required size N is obtained as a connected component without self-loops and multiedges. The (α,β) model generates both edges from/to a new vertex and edges between old vertices, the processes are somewhat analogous to the ones in the generalized Barabási-Albert (BA) model [1,17].

III. SIMULATIONS FOR STOCHASTIC MODEL

We study the typical behavior in the SHIR model on the SF networks. In the following simulations, we set the execution rate $\lambda=0.1$, the detection rate $\delta=0.04$, the average number of edges $\bar{k}=6.6$, and initial infection sources of randomly chosen five vertices (the following results are similar to other small values $\lambda=0.2,0.3$ and $\delta=0.05,0.06$). These small values are realistic, because computer viruses are not recognized before the prevalence and it may be executed by some users. We note the parameters are related to the sharpness of increasing/decreasing infections up/down (δ is more sensitive). It is well known that, in a closed system of the SHIR model, the number of infected computers in the hidden and infectious states is initially increased and saturated, and finally converged to zero as extinction. While the pattern may be different in an open system, indeed, oscillations have been described by a deterministic Kermack-McKendrik model [4]. However, a constant population (equal rates of birth and death) or territorial competition has been mainly discussed in the classical model, the growth of computer network is obviously more rapid, and the communications in mailing are not competitive. Thus, we consider a growing system, in which 50 vertices and the corresponding new $\bar{k}$ edges are added at every step, from an initial SF network with $N=400$ up to 20350 at 400 steps. Here, one step is corresponding to a day (400 steps $\approx$ 1 yr). These values of λ, δ, $\bar{k}$, and the growth rate are only examples with something of reality for simulations, since the actual values that depend on the observed period are still unknown. As shown in Figs. 4(a) and 4(b), the phenomena of persistent recoverable prevalence are found in the open system, but not in the closed system.

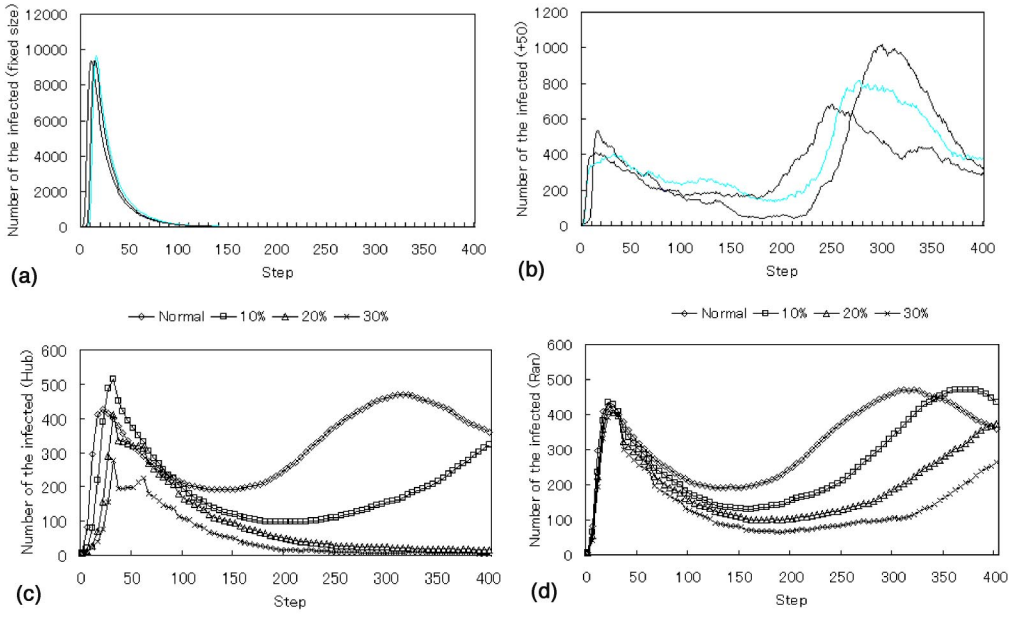

FIG. 4. Typical behavior of the spread on SF networks in (a) a closed system and (b) an open system with simultaneous progress of both spread of viruses and growth of network. The lines show the differences in stochastic state transitions. The effects of immunization are shown as the averages in the open system for (c) hub and (d) random immunization. The open diamond, square, triangle, and cross marks are corresponding to the normal detection by the state transitions, immunization of 10%, 20%, and 30%, respectively.

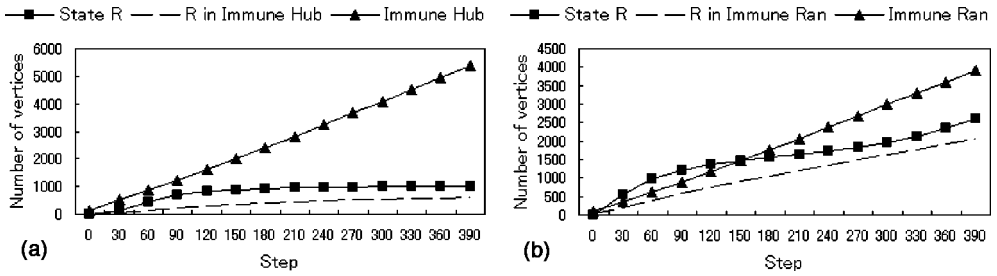

FIG. 5. Number of vertices in the recovered state by (a) hub and (b) random immunization of 30%. Each of them is the average value for recoverable prevalence in 100 trials. The dashed lines represent the number of vertices that are already changed to the recovered states before the immunization.

To prevent the wide spread of infections, we investigate how to assign antivirus software onto the SF networks. We verify the effectiveness of the targeted immunization for hubs even in the cases of recoverable prevalence. Figures 4(c) and 4(d) show the average number of infected computers with recoverable prevalence in 100 trials, where immunized vertices are randomly selected or as hubs according to the out-degree order of 10%, 20%, 30% of growing size at every 30 steps (corresponding to a month). The number is decreased as larger immune rates for hubs, viruses are nearly extinct (there exist only few viruses) in 30% as marked by $\times$ in Fig. 4(c). While it is also decreased as larger immune rates for randomly selected vertices, however they are not extinct even in 30% as marked by $\times$ in Fig. 4(d). Figures 5(a) and 5(b) show the number of recovered states by the hub and random immunization of 30% (triangle marks) for the comparison with the normal detections (rectangle marks). The immunized hubs are more dominant than the normal detections in Fig. 5(a). However, there is no such difference for the random immunization in Fig. 5(b). In the case of 10%, the relation is exchanged; the number of detections is larger than that of both hub and random immunizations. It is intermediate in the case of 20%. From these results, we remark that the targeted immunization for hubs strongly prevents the spread of infections in spite of the fewer totally recovered states than that in random immunization.

IV. ANALYSIS FOR DETERMINISTIC MODEL

Although the stochastic SHIR model is realistic, the analysis is very difficult in the open system. Thus, we analyze simpler deterministic SIR models for the spreading of computer viruses to understand the mechanisms of recoverable prevalence and extinction by immunization. We consider the time evolutions of $S(t)>0$ and $I(t)>0$ $(t\geqslant 0)$, which are the number of susceptible and infected vertices. We assume that infection sources exist in an initial network, and that both network growth and the spread of viruses progress in continuous time as an approximation. In addition, we have no specific rules for growing, but consider a linearly growing network size and the degree distribution on an undirected connected graph as a consequence.

A. Homogeneous SIR model

As the most simple case, in the homogeneous networks with only the detection of viruses, the time evolutions are given by

$$\frac{dS(t)}{dt} = -b\langle k\rangle S(t)I(t) + a, \tag{1}$$

$$\frac{dI(t)}{dt} = -\delta_0 I(t) + b\langle k\rangle S(t)I(t), \tag{2}$$

where $a>0$ and $0<b$, and $\delta_0<1$ denote the growth, infection, and detection rates, respectively. $\langle k\rangle \overset{\text{def}}{=} \Sigma_k kP(k)$ is the average number of connections with a probability $P(k)$ of the degree k. The term $S(t)I(t)$ represents the frequency of contact relations. Note that the number of recovered vertices $R(t)$ is a shadow variable defined by $dR(t)/dt=\delta_0 I(t)$. From the network size $N(t)=S(t)+I(t)+R(t)$, the solution is given by $N(t)=N(0)+at$ as a linear growth. Figure 6(a) shows the nullclines of

$$\frac{dS}{dt}=0: \quad S=\frac{a}{b\langle k\rangle I}$$

and

$$\frac{dI}{dt}=0: \quad S=S^* \overset{\text{def}}{=} \frac{\delta_0}{b\langle k\rangle}, \quad (I\neq 0)$$

for Eqs. (1) and (2). The directions of vector field are defined by the positive or negative signs of dS/dt and dI/dt. There exists a stable equilibrium point (I^*,S^*), $I^* \overset{\text{def}}{=} a/\delta_0$. The

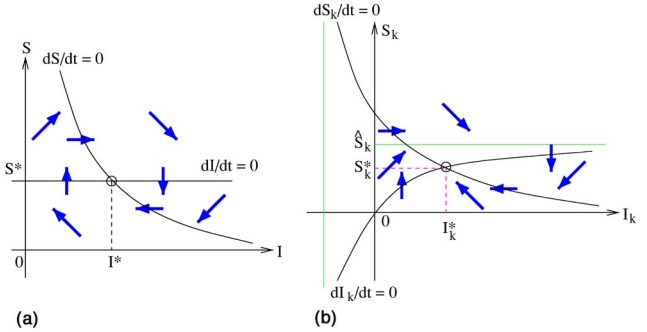

FIG. 6. Nullclines and the vector fields for (a) homogeneous and (b) heterogeneous SIR models. The state in both cases is converged to an equilibrium point with a damped oscillation, which corresponds to persistent recoverable prevalence around the nonzero level I^* or I_k^*.

states of S and I are converged to the point with a damped oscillation. We can easily check that the real parts of eigenvalues for the Jacobian are negative at the point.

B. Heterogeneous SIR model

Next, we consider the heterogeneous SF networks at the mean-field level, in which the connectivity correlations are neglected [18]. We know that static and grown networks have different properties for the size of giant component [19] and the connectivity correlations [20,21] even if the degree distributions are the same. In particular, the correlations may have influence on the spread, however they are not found in all growing network models or real systems. We have experimentally observed that the correlations are very weak in the (α,β) model in the previous simulations similar to the nearest neighbors average connectivity of vertex with k edges in the generalized BA model rather than the fitness model or autonomous system (AS) in the Internet [22]. At least, noncorrelation does not seem to be crucial for the absence of epidemic threshold [3,7,8,18], the existence of correlations is still much less nontrivial in e-mail networks. Although the mean-field approach by neglecting the correlations in macroscopic equations at a large network size is a crude approximation method, it is useful for understanding the mechanisms of the spread in growing networks, as far as it is qualitatively similar to the behavior of viruses in the stochastic model or observed real data. Indeed, the following results are consistent with the analysis for correlated cases [23], except of the quantitative differences.

We introduce a linear kernel [21] as $N_k(t) \sim a_k t, N_k(t) = S_k(t) + I_k(t) + R_k(t)$, which is the sum of the numbers of susceptible, infected, and recovered vertices with degree k, and the growth rate $a_k \stackrel{\text{def}}{=} Ak^{-\nu}, A>0, \nu>2$. Note that the total $N(t) = \Sigma_k N_k(t) \sim (\Sigma_k a_k)t$ means a linear growth of network size. Since the maximum degree increases as the time progresses and approaches to infinity, it has a nearly constant growth rate $\Sigma_{k=m}^{\infty} a_k \sim \int_m^{\infty} Ak^{-\nu} dk = Am^{1-\nu}/(\nu-1)$ for large t. As shown in Ref. [21], the introduction of linear kernel is not a contradiction with the preferential (linear) attachment [1,2].

At the mean-field level in a somewhat large network with only the detection of viruses, the time evolutions of $S_k>0$ and $I_k>0$ are given by

$$\frac{dS_k(t)}{dt} = -bkS_k(t)\Theta(t) + a_k, \tag{3}$$

$$\frac{dI_k(t)}{dt} = -\delta_0 I_k(t) + bkS_k(t)\Theta(t), \tag{4}$$

where the shadow variable $R_k(t)$ is implicitly defined by $dR_k(t)/dt = \delta_0 I_k(t)$. The factor $\Theta(t) \stackrel{\text{def}}{=} \Sigma_k c_k I_k(t), c_k \stackrel{\text{def}}{=} kP(k)/\langle k \rangle$, represents the expectation that any given edge points to an infected vertex.

We consider a section of $I_{k'} = I_{k'}^*$: const. for all $k' \neq k$. Figure 6(b) shows the nullclines of

$$\frac{dS_k}{dt} = 0: \quad S_k = \frac{a_k}{kb\Theta} = \frac{a_k}{kbc_k I_k + kb\sum_{k'} c_{k'} I_{k'}^*},$$

$$\frac{dI_k}{dt} = 0: \quad S_k = \frac{\delta_0 I_k}{kb\Theta} = \frac{\delta_0 I_k}{kbc_k I_k + kb\sum_{k'} c_{k'} I_{k'}^*},$$

and the vector field for Eqs. (3) and (4). There exists a stable equilibrium point $(I_k^*, S_k^*) \stackrel{\text{def}}{=} (a_k/\delta_0, a_k/kb\Theta^*)$, because of

$$\exists \Theta^* = \sum_{k \geqslant m} c_k I_k^* \sim \frac{A\gamma m^{-\gamma}}{\delta_0} \int_m^{\infty} k^{-(\nu+\gamma+1)} dk = \frac{A\gamma m^{-\nu}}{\delta_0(\nu+\gamma)},$$

by using $c_k = \gamma \times m^{\gamma} \times k^{-(\gamma+1)}$ for the generalized BA model [18] with a power-law degree distribution $P(k) = (1+\gamma)m^{1+\gamma}k^{-2-\gamma}, \langle k \rangle = m(1+\gamma)/\gamma$ (which includes the simple BA model [2] at $\gamma = 1$). On these state spaces in Figs. 6(a) and 6(b), only the case of $a=0$ or $a_k=0$ gives the extinction: $I^*=0$ or $I_k^*=0$. It means that we must stop the growth to prevent the infections by detection. In addition, the homogeneous and heterogeneous systems are regarded as oscillators in Figs. 7(a) and 7(b).

C. Effect of immunization

We study the effect of random and hub immunization. With the randomly immune rate $0<\delta_r<1$, the time evolutions are given by

$$\frac{dS_k(t)}{dt} = -bkS_k(t)\Theta(t) + a_k - \delta_r S_k(t), \tag{5}$$

$$\frac{dI_k(t)}{dt} = -\delta_0 I_k(t) + bkS_k(t)\Theta(t) - \delta_r I_k(t), \tag{6}$$

where the shadow variable $R_k(t)$ is defined by $dR_k(t)/dt = \delta_0 I_k(t) + \delta_r(S_k(t) + I_k(t))$.

Similar to discussions in the preceding section, we consider a section of $I_{k'} = I_{k'}^*$: const for all $k' \neq k$. From the nullclines of Eqs. (5) and (6) with random immunization, there exists a stable equilibrium point $(I_k^*, S_k^*) \stackrel{\text{def}}{=} [(a_k - \delta_r S_k^*)/(\delta_0 + \delta_r), a_k/(\delta_r + kb\Theta^*)]$, if the solution

$$\Theta^* = \sum_k c_k I_k^* = \frac{1}{\delta_0 + \delta_r} \sum_k a_k c_k \left(1 - \frac{\delta_r}{\delta_r + bk\Theta^*}\right) \stackrel{\text{def}}{=} f(\Theta^*)$$

is self-consistent at the point. The condition is given by

$$\left.\frac{df}{d\Theta}\right|_{\Theta=0} \approx \frac{Ab}{\delta_r(\delta_0+\delta_r)} \int_m^{\infty} \gamma m^{\gamma} k^{-(\gamma+\nu)} dk = \frac{Ab\gamma m^{-(\nu-1)}}{\delta_r(\delta_0+\delta_r)(\gamma+\nu-1)} > 1.$$

In this case, the state space is the same as shown in Fig. 6(b).

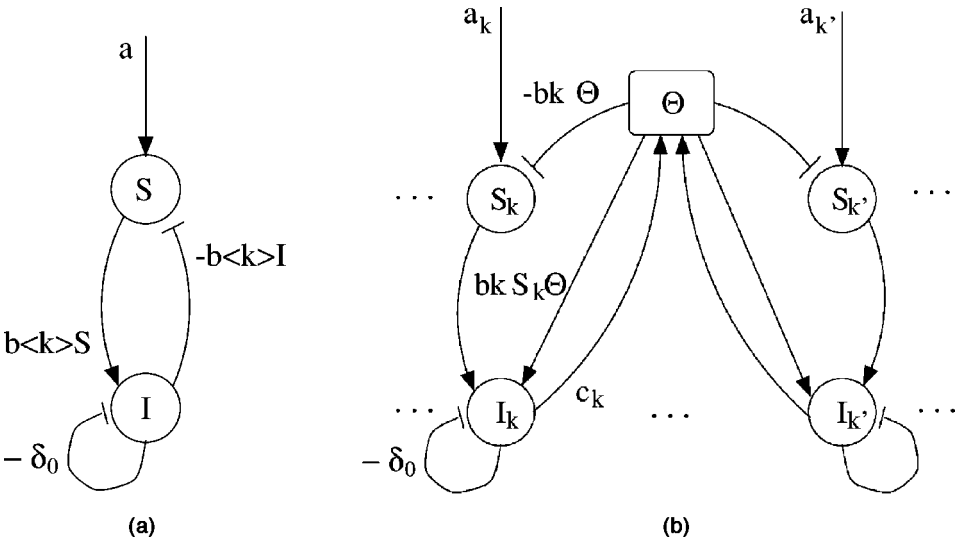

FIG. 7. Oscillators for (a) homogeneous and (b) heterogeneous SIR models in the open system. They consist of S-I pairs with excitatory → and inhibitory ⊣ connections, and an input bias a or a_k of the growth rate. The factor Θ acts as a global inhibition or excitation.

Next, we assume $I^*_{k'}=0$ for all $k'\neq k$ to discuss the extinction. On this section, the nullclines are

$$\frac{dS_k}{dt}=0: \quad S_k=\frac{a_k}{\delta_r+kb\Theta}=\frac{a_k}{\delta_r+kbc_kI_k}$$

and

$$\frac{dI_k}{dt}=0: \quad S_k=\frac{(\delta_0+\delta_r)I_k}{kb\Theta}=\frac{\delta_0+\delta_r}{kbc_k} \quad (I_k\neq 0)$$

for Eqs. (5) and (6). The necessary condition of extinction is given by the fact that the point $(0,a_k/\delta_r)$ on the nullcline $dS_k/dt=0$ is below the line $S_k=(\delta_0+\delta_r)/kbc_k$: const of $dI_k/dt=0$. From the condition

$$\frac{a_k}{\delta_r}<\frac{\delta_0+\delta_r}{kbc_k},$$

we obtain

$$\delta_r>-\delta_0+\sqrt{\delta_0^2+4ka_kbc_k}. \tag{7}$$

In addition, since $0<\delta_r<1$ must be satisfied, it is given by $a_k<(1+2\delta_0)/4b\gamma$ from $kc_k=\gamma m^\gamma k^{-\gamma}$, $m\leqslant k<\infty$, $\gamma>0$, for the generalized BA model [18]. In this case, there exists a stable equilibrium point, otherwise a saddle and a stable equilibrium point as shown in Figs. 8(a) and 8(b). The state space is changed through a saddle-node bifurcation by values of the growth rate a_k and the immune rate δ_r.

For the hub immunization [7], δ_r is replaced by $0<\delta_h k^\tau<1, \tau>0$, e.g., $\tau=1$ as proportional immunization to the degree of vertex. We may choose $1/k^\tau$ times smaller immune rate δ_h than δ_r for Eq. (7). In other words, the necessary condition of extinction in Eq. (7) is relaxed to $a_k<m^\tau(m^\tau+2\delta_0)/4b\gamma$. Thus viruses can be removed in larger growth rate.

The above conditions are almost fitting to the results for the stochastic model in Sec. III. We can evaluate them using the corresponding parameters $m=1$, $\nu=2+\gamma=(\gamma_{in}+\gamma_{out})/2=2.2$, $b\leftrightarrow\lambda=0.1$, $\delta_0\leftrightarrow\delta=0.04$, δ_r or $\delta_h=0.1,0.2,0.3$, $\tau=1$, and $A=60$ from $(\Sigma a_k)\sim\int Ak^{-\nu}dk=Am^{1-\nu}/\nu-1=50$. By simple calculations, we find that $a_k<(1+2\delta_0)/4b\gamma$ is satisfied for $k\geqslant 2$. The condition (7) is satisfied for only $k\geqslant 5$ with random immunization of 30% and $k\geqslant 7$ with 20%, so the extinction of viruses is difficult by spreading of infection from many vertices with low degree $k\leqslant 4$, whereas it is satisfied for $k\geqslant 3$ with hub immunization of both 20% and 30% by the factor of $1/k^\tau$. The delicate mismatch at $k=1,2$ may be from the difference of the complicated stochastic behavior as in Fig. 1 and the macroscopic crude approximation.

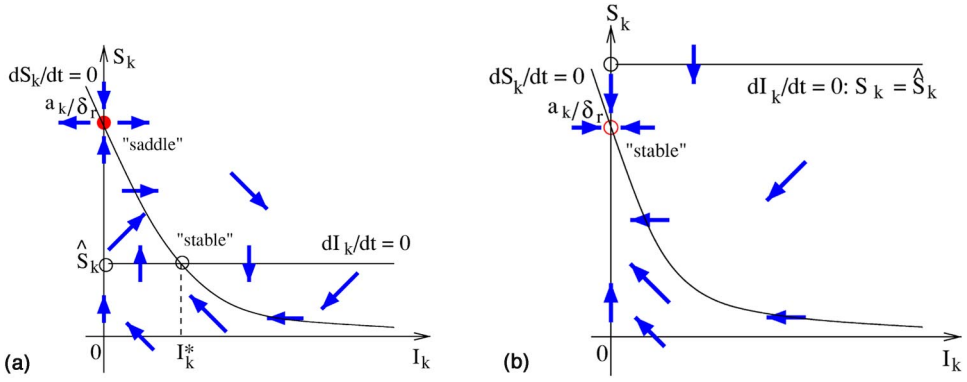

FIG. 8. Saddle-node bifurcation between (a) damped oscillation of recoverable prevalence and (b) convergence to the extinction by the immunization in the heterogeneous SIR model. The state space is changed by the bifurcation parameters δ_r and a_k for the value of $\hat{S}_k\overset{\text{def}}{=}(\delta_0+\delta_r)/kbc_k$.

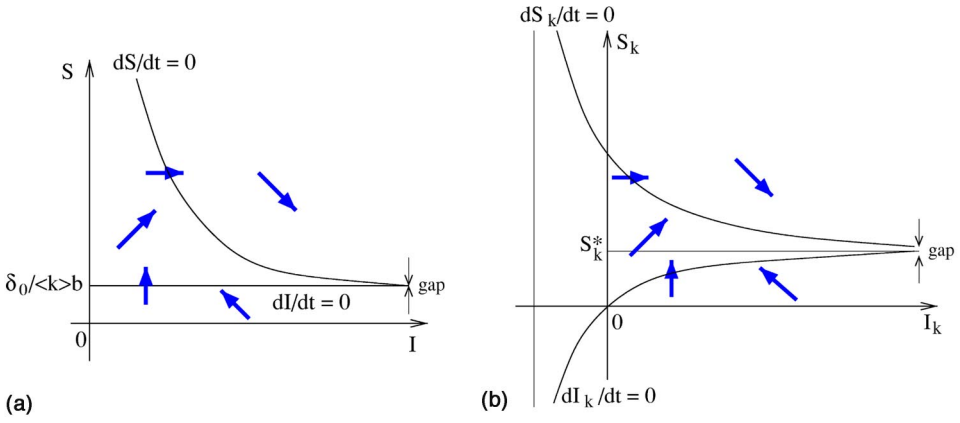

FIG. 9. Nonextinction in (a) homogeneous and (b) heterogeneous SIS models. The number of infected state I or I_k finally diverges to infinity.

D. SIS model

Finally, to show that the recovered state is necessary, we consider the SIS models in the open system. The time evolutions on homogeneous networks are given by

$$\frac{dS(t)}{dt} = \delta_0 I(t) - b\langle k\rangle S(t) I(t) + a, \tag{8}$$

$$\frac{dI(t)}{dt} = -\delta_0 I(t) + b\langle k\rangle S(t) I(t), \tag{9}$$

where $N(t) = S(t) + I(t)$. The nullclines are

$$\frac{dS}{dt} = 0: \quad S = \frac{\delta_0 I + a}{b\langle k\rangle I} = \frac{\delta_0}{b\langle k\rangle} + \frac{a}{b\langle k\rangle I}$$

and

$$\frac{dI}{dt} = 0: \quad S = \frac{\delta_0}{b\langle k\rangle} : \text{const}, (I \neq 0)$$

for Eqs. (8) and (9). There exists a gap of $a/b\langle k\rangle I > 0$ even in $I^* \to \infty$. Furthermore, the time evolutions on heterogeneous networks are given by

$$\frac{dS_k(t)}{dt} = \delta_0 I_k(t) - bkS_k(t)\Theta(t) + a_k, \tag{10}$$

$$\frac{dI_k(t)}{dt} = -\delta_0 I_k(t) + bkS_k(t)\Theta(t). \tag{11}$$

On a section $I_{k'}$: const, the nullclines are

$$\frac{dS_k}{dt} = 0: \quad S_k = \frac{\delta_0 I_k + a_k}{kb\Theta} \quad \text{and} \quad \frac{dI_k}{dt} = 0: \quad S_k = \frac{\delta_0 I_k}{kb\Theta}$$

for Eqs. (10) and (11). There also exists a gap between the nullclines. Figures 9(a) and 9(b) show the nullclines and the vector field. Thus, the dynamics in the SIS model is quite different from that in the SIR model. We cannot realize both the extinction and the recoverable prevalence of viruses on the SIS model, in any case, even in the open system.

V. CONCLUSION

In summary, we have investigated the spread of computer viruses via e-mails on linearly growing SF network models whose exponents of the degree distributions are estimated from real data of sent and received mails [13] or from the generalized BA model [1,18]. The dynamic behavior is the same in both simulations for a realistic stochastic SHIR model and a mean-field approximation without connectivity correlations for the macroscopic equations of simpler deterministic SIR models. The obtained results suggest that the recoverable prevalence stems from the growth of network, and it is bifurcated from the extinction state according to the relations of growth, infection, and immune rates. Moreover, the targeted immunization for hubs is effective even in the growing system. Quantitative fitness with really observed virus data and more detailed analysis with the correlations are further studies.

[1] R. Albert and A.-L. Barabási, e-print cond-mat/0106096.
[2] A.-L. Barabási, R. Albert, and H. Jeong, Physica A **272**, 173 (1999).
[3] R. Pastor-Satorras and A. Vespignani, Phys. Rev. E **63**, 066117 (2001).
[4] N. Shigesada and K. Kawasaki, *Biological Invasions: Theory and Practice* (Oxford University Press, Oxford, 1997).
[5] R.M. May and A.L. Lloyd, Phys. Rev. E **66**, 066112 (2001).
[6] M.E.J. Newman, Phys. Rev. E **65**, 016128 (2002).
[7] Z. Dezsö and A.L. Barabási, Phys. Rev. E **65**, 055103 (2002).
[8] R. Pastor-Satorras and A. Vespignani, Phys. Rev. E **65**, 036104 (2002).
[9] R. Albert, H. Jeong, and A.-L. Barabási, Nature (London) **406**, 378 (2000).
[10] See http://sophy.asaka.toyo.ac.jp/users/mikami/info&media/, http://www.commerce.or.jp/result/sp3/index.html, http://www.dentsu.co.jp/marketing/digital_life/
[11] J. O. Kephart and S. R. White, *Proceedings of the 1993 IEEE Coimputer Society Symposium on Security and Privacy* (IEEE, Washington, 1993), pp. 2–15.

[12] S. R. White, J. O. Kephart, and D. M. Chess, Proceedings of the Fifth Virus Bulletin International Conference, 1995 (unpublished); see http://www.research.ibm.com/antivirus/SciPapers/white/VB95/vb95.distrib.html
[13] See http://www.theo-physik.uni-kiel.edu/~ebel/email-net/email-net.html.
[14] H. Ebel, L.-I. Mielsch, and S. Bornholdt, Phys. Rev. E **66**, 035103(R) (2002).
[15] M.E.J. Newman, S. Forrest, and J. Balthrop, Phys. Rev. E **66**, 035101 (2002).
[16] R. Kumar *et al.*, Proceedings of the 25th VLDB Conference, 1999 (unpublished), pp. 639-650; see http://www.almaden.ibm.com/cs/people/ravi/papers.html
[17] R. Albert and A.-L. Barabási, Phys. Rev. Lett. **85**, 5234 (2000).
[18] Y. Moreno, R. Pastor-Satorras, and A. Vespignani, Euro. Phys. J. **26**, 521 (2002).
[19] S.N. Dorogovtsev, J.F.F. Mendes, and A.N. Samukhin, Phys. Rev. E **64**, 066110 (2001).
[20] D.S. Callaway *et al.*, Phys. Rev. E **64**, 041902 (2001).
[21] P.L. Krapivsky and S. Redner, Phys. Rev. E **63**, 066123 (2001).
[22] R. Pastor-Satorras, A. Vázquez, and A. Vespignani, Phys. Rev. Lett. **87**, 258701 (2001).
[23] Y. Hayashi, e-print cond-mat/0307135.